Al-Azhar Engineering 16th International Conference

Vol. 19, No. 72, July 2024, 56 - 74

INVESTIGATION OF STATIC AND DYNAMIC BEHAVIOR OF PROPORTIONAL FLOW CONTROL VALVE PROVIDED BY PRESSURE COMPENSATOR

M. Gomaa Aboalnagah[1*], Ziad A. Ibrahim[2], M.Elfaisal Elrefaie[1]

[1] Mechanical engineering department , Faculty of Engineering, Al-Azhar University, Nasr City, 11884, Cairo, Egypt

[2] Mechanical engineering department, Faculty of Engineering ,Future University, Cairo, Egypt

***Correspondence:** Mohamedaboalnaga89@gmail.com

Citation:

M.G. Aboalnagah , Z.A. Ibrahim and M.E. Elrefaie, "Investigation of the static and dynamic behavior of proportional flow control valve provided by pressure compensator", Journal of Al-Azhar University Engineering Sector, vol. 19, pp. 56 - 74, 2024

Received: 09 November 2023

Revised: 26 December 2023

Accepted: 31 December 2023

DOI:10.21608/auej.2023.247530.1466

ABSTRACT

Infinitely controlled operating fluid flux can be obtained in hydraulic circuits for fluid power systems by the presence of flow control valves of proportional type before hydraulic actuators. This research introduces a detailed mathematical model for a class of pressure-compensated proportional flow control valves. The numerical values of the construction parameters for the mentioned valve were obtained from the disassembly of the valve and conducting the necessary measurements, as well as the manufacturer's technical data sheet. The static and dynamic behavior of the valve at different conditions is investigated by a simulation program constructed by the MATLAB SIMULINK package. An experimental setup was constructed to evaluate model steady-state fluid flux. The simulated steady-state valve flow rate satisfactorily agrees with the experimental results. The effect of the variation of load pressure, supply pressure, and valve construction parameters is considered. The studied parameters are downstream valve spool spring stiffness, downstream compensator spring stiffness, spring pre-compression, compensator damping hole diameter, and compensator mass. The present results indicate that the controlled flow rate increases as compensator spring stiffness or pre-compression increases and as valve spool spring stiffness decreases. Increasing the compensator damping orifice diameter leads to a decrease in the transient time. The compensator mass has no significant impact on the transient time.

KEYWORDS: Proportional flow control valve, Pressure compensator, MATLAB SIMULINK, mathematical model, Solenoid.

فحص الأداء الإستاتيكي والديناميكي لصمام التحكم في التصرف من النوع التناسبي المزود بمنظم للضغط

محمد جمعه أبوالنجاه [1*]، زياد أحمد إبراهيم[2] ، محمد الفيصل الرفاعي[1]

[1]قسم الهندسة الميكانيكة ، كلية الهندسة، جامعة الأزهر، مدينة نصر، 11884، القاهرة، مصر.

[2]قسم الهندسة الميكانيكة ، كلية الهندسة، جامعة المستقبل ، القاهرة، مصر.

***البريد الاليكتروني للباحث الرئيسي :** Mohamedaboalnaga89@gmail.com

الملخص

يمكن الحصول على تدفق مائع التشغيل الذي يتم التحكم فيه بشكل لا نهائي في الدوائر الهيدروليكية لأنظمة نقل الحركة من خلال وجود صمامات التحكم في التدفق من النوع التناسبي قبل المشغلات الهيدروليكية. يقدم هذا البحث نموذجاً رياضياً مفصلاً لفئة من صمامات التحكم في التدفق من النوع التناسبي المنظم للضغط. تم الحصول على القيم العددية لأبعاد ومعلمات الصمام المذكور من خلال تفكيك الصمام وإجراء القياسات اللازمة، بالإضافة إلى ورقة البيانات الفنية للشركة المصنعة. تم فحص الأداء الإستاتيكي والديناميكي للصمام في ظروف التشغيل المختلفة من خلال برنامج محاكاة تم إنشاؤه بواسطة حزمة MATLAB SIMULINK. تم إنشاء تزجة إختبار لقياس معدل السريان في الحالة المستقرة لمائع التشغيل الذي تم الحصول عليه نظريا من برنامج المحاكاه. ويتفق معدل تدفق صمام الحالة المستقرة المحاكى بشكل مرض مع النتائج المعملية. تم أخذ تأثير اختلاف الضغط قبل وبعد الصمام ومعلمات بناء الصمام في الاعتبار. المعلمات التي تمت دراستها هي صلابة زنبرك زلاق الصمام ، وصلابة زنبرك زلاق منظم الضغط، وطول إنضغاطه الإبتدائي، وقطر فتحة الخامد الموجود بزلاق منظم الضغط، وكتلة زلاق منظم الضغط. تشير النتائج الحالية إلى أن دقة معدل التدفق المتحكم فيه يزداد مع زيادة صلابة زنبرك منظم الضغط، أو الضغط المسبق وكذلك مع انخفاض صلابة زنبرك زلاق الصمام. تؤدي زيادة قطر فتحة الخامد الموجود بزلاق منظم الضغط إلى انخفاض الزمن اللازم للوصول لحالة الإستقرار.وتشير النتائج أيضا الي أنه ليس لكتلة منظم الضغط، أي تأثير كبير على الزمن اللازم للوصول لحالة الإستقرار.

الكلمات المفتاحية : صمام التحكم في التصرف من النوع التناسبي، منظم الضغط، MATLAB SIMULINK، النموذج الرياضي، الملف اللولبي

1. INTRODUCTION

The development of proportional valve designs by researchers, research centers, and manufacturers is considered a technical solution to complex hydraulic circuits[1-6]. These valve families allow unlimited valve spool positioning, thus providing infinitely adjustable flow volumes[7-10]. Either stroke-controlled or force-controlled solenoids are used to achieve the infinite positioning of the valve spool [11- 16].Available variable positioning for the spool allows for varying valve metering notches to provide flow and then speed control. Proportional valves are controlled by changing an electrical signal that controls the stroke of the valve spool over metering ports. This produces a variable flow of fluid, thereby providing the ability to vary the flowrate and then the speed of the actuator being controlled.

The present work introduces a complete, detailed mathematical model for a certain type of proportional flow control valve (PFCV). The mathematical model considered all the non-linear effects in the PFCV. The mathematical model considered the friction effec, the non-linear relation of the change of the throttling areas with the displacement of the spools, and the effect of compressibility when applying the continuity equation through the different cavities and pipe lines connected to the valve. We get a high-fidelity model to simulate the static and dynamic behavior of the valve in reality.

The simulation model, based on the deduced mathematical equations, provides researchers and manufacturers with a good understanding of the valve behavior of both transient and steady-state conditions, which can help to manufacture new families of valve works in different flowrates and different working pressures.

A validated study model is important for manufacturers because an understanding of the model design key points can be used to modify the studied valve characteristics by varying valve construction parameters. The simulation model will help in the design of a hydrostatic transmission system used as part of a hydraulic control system in wind turbines. According to the performance of the studied valve, we have constant flow rates to the hydraulic motor, which rotates the synchronous generator in spite of the varying loading conditions. The presence of the studied valve in the designed system reduces the required control elements. also ensuring continued operation and constant electric power generation in the case of low turbine speeds [17].

The selected valve (Duplomatic QDE5-80/10N-D24K1) [18] shown in **Fig**. **1** consists basically of housing (1), force-controlled proportional solenoid (2), The flow (from port P to B) passes through the compensator throttling area (8) after the valve throttling restriction (7) ,which is located in the wall of the valve spool (3). The valve spool is loaded by the downstream valve spring (4). Pressure compensator (5), loaded by downstream compensator spring (6). The setting of the flow is determined by setting the input command signal.

At certain input command value, the proportional solenoid core is attracted and moves to the right. The main throttling orifice is open, which means the valve spool moves to the right against the downstream valve spring until the valve spool has displaced the equal distance produced by the proportional solenoid according to the input command value "the valve spool rested on the proportional solenoid core". At the same time, the compensator moves to the left by the downstream compensator spring. The displacement of the compensator to the left increases the exit throttling area, which is machined in compensator on the right side. This position allows the operating fluid to flow from the inlet chamber to the port (B).

If the supply pressure is increased, the flow rate increases. Simultaneously, the compensator moves to the right against the downstream compensator spring. This displacement is produced by the pressure force against the spring force caucus decreases the exit area of the compensator restriction. The compensator kept the pressure difference between the valve inlet and exit constant by using a damping hole, which is a tube machined inside the compensator. Thus, the valve again reaches a steady state and maintains a constant flow rate.

If the supply pressure is decreased, the flow rate (Q_m) decreases. The pressure force inside the inlet chamber acting on the compensator becomes less than the downstream compensator spring force. The spring pushes the compensator to the left, increasing the exit restriction area. The flow rate and the pressure difference increase until they reach the required steady-state values again.

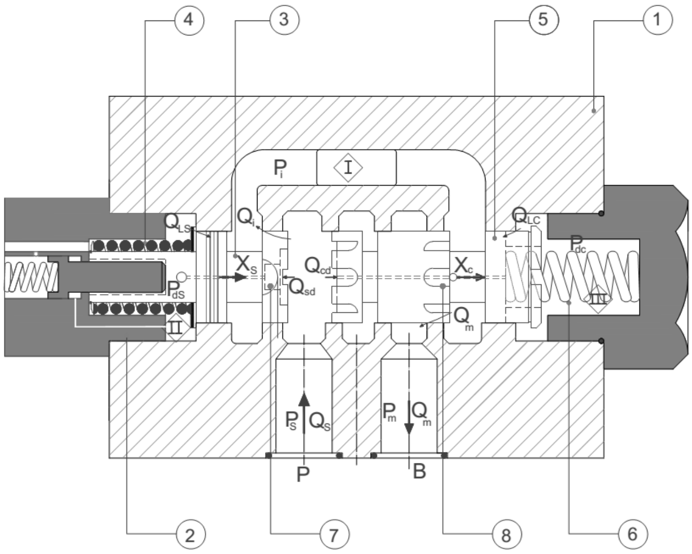

Fig.1. Schematic drawing of the studied valve

2. MATHEMATICAL MODEL

The mathematical model for the selected valve is solved numerically to obtain the dynamic behavior of this valve. Equations describing the dynamic behavior of the selected element are deduced as follows:

Equations of Motion

The core of the valve moves under the action of the spring force (F_{se}), seat reaction forces (F_{SR1}, F_{SR3}), viscous friction force (F_{ef}).and the solenoid force applied to the core (F_e), as shown in **Fig**.2.

The dynamic equation of motion of the core is as follows:

$$\frac{d^2X_e}{dt^2} = \frac{1}{m_e}\left[F_e - F_{SR1} - F_{SR3} - F_{ef} + F_{se}\right] \tag{1}$$

Where, m_e ,and X_e are core mass(kg), core displacement(m), respectively.

Solenoid force applied to the core (F_e) can be obtained from following transfer function [19-21]

$$F_e(s) = G * \frac{\omega_n{}^2}{S^2 + 2\zeta\omega_n S + \omega_n{}^2}\ I(s) \tag{2}$$

Where, I is PFCV input current(A), respectively.

$$F_{Se} = K_{se}\ (X_e + X_{e0}) \tag{3}$$

Where, K_{se} , and X_{e0} are core spring stiffness(N/m), and downstream core spring pre-compression(m) , respectively.

$$F_{ef} = f\frac{dX_e}{dt} \tag{4}$$

Where, f, is Friction coefficient (Ns/m).

$$F_{SR1} = \begin{cases} o & X_e \le \text{stroke} \\ K\,|X_e| - R\frac{dX_e}{dt} & X_e \ge \text{stroke} \end{cases} \tag{5}$$

Where, K, and R are equivalent seat material stiffness(N/m), and equivalent seat material damping coefficient(N. s/m), respectively.

$$F_{SR3} = \begin{cases} o & X_e < X_s \\ K\,|X_e - X_s| + R\frac{d(X_e - X_s)}{dt} & X_e \ge X_s \end{cases} \tag{6}$$

Where, X_s is valve spool displacement(m).

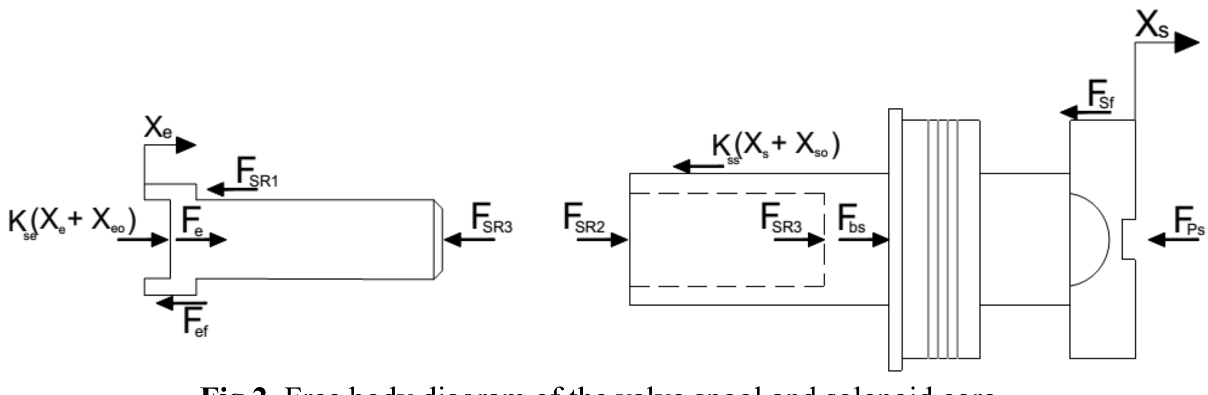

Fig.2. Free body diagram of the valve spool and solenoid core

The valve spool moves under the action of the spring force (F_{ss}), seat reaction forces (F_{SR2}, F_{SR3}), pressure forces (F_{Ps}, F_{bs}) and the viscous friction force (F_{sf}).The dynamic equation of motion of the valve spool is as follows:

$$\frac{d^2X_s}{dt^2} = \frac{1}{m_s}\left[\,F_{bs} + F_{SR3} + F_{SR2} - F_{ss} - F_{Ps} - F_{Sf}\right] \tag{7}$$

Where, m_s is valve spool mass(kg).

$$F_{SS} = K_{ss}\ (X_s + X_{s0}) \tag{8}$$

Where, K_{ss}, and X_{s0} are downstream valve spool spring stiffness(N/m), and downstream valve spool spring pre-compression (m), respectively.

$$F_{sf} = f\frac{dX_s}{dt} \quad ,\text{where } f = \mu\frac{A_{ps}}{c} \;,\; A_{ps} = \pi D_s L_{sh} \tag{9}$$

Where, μ, c, A_{ps}, D_s, and L_{sh} are oil dynamic viscosity coefficient (Pa.s), radial clearance (m), valve spool side area (m^2), valve spool diameter (m), and contact distance between valve spool and housing (m), respectively.

$$F_{SR2} = \begin{cases} 0 & X_s \geq 0 \\ K\,|X_s| - R\frac{dX_s}{dt} & X_s \leq 0 \end{cases} \tag{10}$$

$$F_{Ps} = P_s\,.A_s \qquad , A_s = \frac{\pi}{4}(D_s)^2 \tag{11}$$

Where, P_s, and A_s are upstream pressure applied in valve spool (Pa), and valve spool cross section area (m^2), respectively.

$$F_{bs} = P_{ds}\,.A_s \tag{12}$$

Where, P_{ds} is downstream pressure applied on valve spool(Pa).

The compensator spool moves under the action of the spring force (F_{sc}), seat reaction force (F_{SR4}), pressure forces (F_{Ps}, F_{bc}) and viscous friction force (F_{cf}) , as referred to in **Fig.3.**

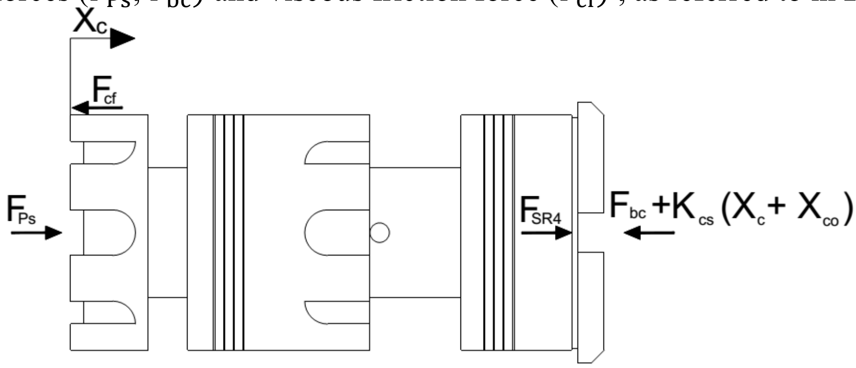

Fig.3. Compensator spool free body diagram

The equation of motion of the pressure compensator spool is given as follows:

$$\frac{d^2X_c}{dt^2} = \frac{1}{m_c}\left[F_{Ps} + F_{SR4} - F_{bc} - F_{Sc} - F_{cf}\right] \tag{13}$$

Where, m_c ,and X_c are compensator mass (kg), compensator spool displacement (m), respectively.

$$F_{Sc} = K_{cs}\,(X_c + X_{c0}) \tag{14}$$

Where, K_{cs} , and X_{c0} are downstream compensator spring stiffness (N/m), and downstream compensator spring pre-compression (m), respectively.

$$F_{cf} = f\frac{dX_c}{dt} \quad , \quad \text{where } f = \mu\frac{A_{pc}}{c}, A_{pc} = \pi D_c L_{ch} \tag{15}$$

Where, A_{pc}, D_c, and L_{ch} are compensator side area (m^2), compensator diameter (m), and contact distance between compensator and housing(m), respectively.

$$F_{SR4} = \begin{cases} 0 & X_c \geq 0 \\ K\,|X_c| - R\frac{dX_c}{dt} & X_c \leq 0 \end{cases} \tag{16}$$

$$F_{Pc} = P_s \cdot A_c \qquad , A_c = \frac{\pi}{4} (D_c)^2 \tag{17}$$

Where, A_c is compensator cross section area (m^2).

$$F_{bc} = P_{dc} \cdot A_{oc} \qquad , A_{oc} = \frac{\pi}{4} (D_c)^2 \tag{18}$$

Where, P_{dc} is downstream pressure applied on compensator spool (Pa).

Throttling areas are calculated as follows,

The spool and compensator restriction are machined such that the area opened is of half-circle shape. **Fig. 4A**. Shows one of four orifices that represent the area A_i .The opened area is deduced as follows:

$$A_i = \pi\, r_i^2 . \frac{\theta}{360} - (r_i - X_s)\sqrt{r_i^2 - (r_i - X_s)^2} \tag{19A}$$

$$A_i = \pi\, r_i^2 . \frac{\theta}{360} - (r_i - X_s)\sqrt{2 r_i X_s - X_s^2} \tag{19B}$$

$$\frac{\theta}{2} = \cos^{-1}\left(\frac{(r_i - X_s}{r_i}\right) \tag{19C}$$

$$A_i = \pi\, r_i^2 . \frac{2\cos^{-1}\left(\frac{(r_i - X_s}{r_i}\right)}{360} - (r_i - X_s)\sqrt{2 r_i X_s - X_s^2} \tag{19D}$$

$$A_i = \begin{cases} o & X_s \le X_d \\ 4\left[\frac{\pi r_i^2}{180} . \cos^{-1}\left(\frac{(r_i - X_s}{r_i}\right) - (r_i - X_s)\sqrt{2 r_i X_s - X_s^2}\,\right] & X_s \ge X_d \end{cases} \tag{19}$$

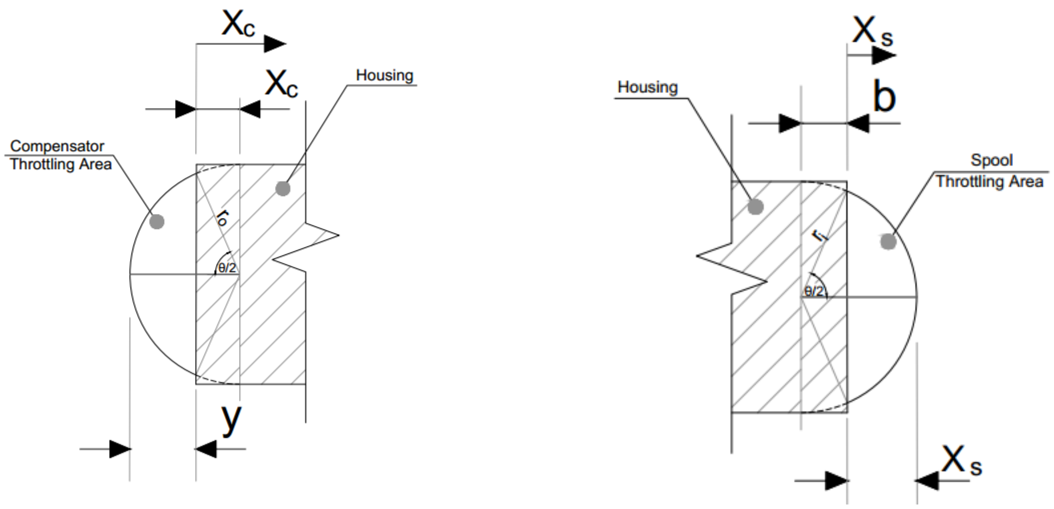

Fig.4B. Pressure compensator restriction area **Fig.4A**. valve spool throttling area

Figure 4B. Shows one of eight orifices that represent the area A_o. An expression for this area is deduced as follows:

$$A_o = \pi\, r_o^2 . \frac{\theta}{360} - X_c\sqrt{r_o^2 - X_c^2} \tag{20A}$$

$$\frac{\theta}{2} = \cos^{-1}\left(\frac{X_c}{r_o}\right) \tag{20B}$$

$$A_o = \pi\, r_o^2 . \frac{2\cos^{-1}\left(\frac{X_c}{r_o}\right)}{360} - X_c\sqrt{r_o^2 - X_c^2} \tag{20C}$$

$$A_o = \begin{cases} 0 & X_c \geq r_O \\ 8[\frac{\pi . r^2}{180} . \cos^{-1}(\frac{X_c}{r}) - X_c\sqrt{r^2 - {X_c}^2}\,] & X_c \leq r_O \end{cases} \quad (20)$$

The flow rates through the valve areas are:

The compensator damping orifice is a short tube orifice **Fig.5** .The flow rates through the compensator damping orifice from the inlet chamber to the intermediate chamber and downstream compensator spring chamber are deduced as follows:

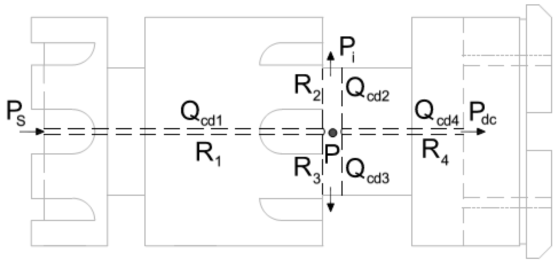

Fig.5. Compensator spool damping holes details

$$Q_{cd1} = Q_{cd2} + Q_{cd3} + Q_{cd4} \quad (21A)$$

Where, Q_{cd1},Q_{cd2}, Q_{cd3}, and Q_{cd4} are flow rates through compensator damping holes (m^3/sec).

$$Q_{cd1} = 2Q_{cd2} + Q_{cd4} \qquad \text{where, } Q_{cd2} = Q_{cd3} \quad (21)$$

$$P_s - P = R_1 Q_{cd1} \qquad \text{where, } R_1 = \frac{128\,\mu.\,L_{cd1}}{\pi.d_{cd1}^4} \quad (22)$$

Where, P,R1, μ, L_{cd}, and d_{cd} are damping holes intersection point pressure (Pa) , hydraulic pass resistance (Pa.s/m^3), oil dynamic viscosity coefficient (Pa.s), compensator damping hole length (m), and compensator damping hole diameter (m) , respectively.

$$P - P_i = R_2 Q_{cd2} \qquad \text{where, } R_2 = \frac{128\,\mu.\,L_{cd2}}{\pi.d_{cd2}^4} \quad (23A)$$

Where, P_i is PFCV intermediate chamber pressure (Pa).

$$P - P_i = R_3 Q_{cd3} \quad (23B)$$

By sum. Eqs. (23A), (23B), the following relation is obtained:

$$2(P - P_i) = R_2 Q_{cd2} + R_3 Q_{cd3} \qquad \text{where, } R_2 = R_3 \;,\; Q_{cd2} = Q_{cd3} \quad (23C)$$

Eq. (23C) can be re- rewriting as follows,

$$P - P_i = R_2 Q_{cd2} \quad (23)$$

$$P - P_{dc} = R_4 Q_{cd4} \qquad \text{where, } R_4 = \frac{128\,\mu.\,L_{cd4}}{\pi.d_{cd4}^4} \quad (24)$$

By substituting Eqs. (23), (21) in eq. (22), the following relation is obtained:

$$P_s - P_i = R_2 Q_{cd2} + 2R_1 Q_{cd2} + R_1 Q_{cd4} \quad (25)$$

By substituting Eq. (24) in eq. (22), the following relation is obtained:

$$P_s - P_{dc} = R_4 Q_{cd4} + 2R_1 Q_{cd2} + R_1 Q_{cd4} \quad (26)$$

Eq. (26) can be re rewriting as follows,

$$Q_{cd2} = \frac{1}{2R_1}[\,(P_s - P_{dc}\,) - Q_{cd4}(R_1 + R_4)] \quad (27)$$

Where, P_{dc} is compensator downstream chamber pressure (Pa).

By substituting Eq. (27) in eq. (25), the following relation is obtained:

$$P_s - P_i = \frac{2R_1 + R_2}{2R_1}[(P_s - P_{dc}) - Q_{cd4}(R_1 + R_4)] + R_1 Q_{cd4} \qquad (28A)$$

In rearrangement Eq. (28A), the following relations are obtained:

$$\frac{2R_1}{2R_1 + R_2}(P_s - P_i) = [(P_s - P_{dc}) - Q_{cd4}(R_1 + R_4)] + \frac{2{R_1}^2}{2R_1 + R_2}Q_{cd4} \qquad (28B)$$

$$\frac{2R_1}{2R_1 + R_2}(P_s - P_i) - (P_s - P_{dc}) = \frac{2{R_1}^2 - (2R_1 + R_2)(R_1 + R_4)}{2R_1 + R_2}Q_{cd4} \qquad (28C)$$

$$Q_{cd4} = \frac{2R_1 + R_2}{2{R_1}^2 - (2R_1 + R_2)(R_1 + R_4)}[\frac{2R_1}{2R_1 + R_2}(P_s - P_i) - (P_s - P_{dc})] \qquad (28D)$$

$$Q_{cd4} = I[J(P_s - P_i) - (P_s - P_{dc})] \qquad (28)$$

Where,

$$I = \frac{2R_1 + R_2}{2{R_1}^2 - (2R_1 + R_2)(R_1 + R_4)} \quad , \quad J = \frac{2R_1}{2R_1 + R_2}$$

$$Q_{cd2} = w[(P_s - P_{dc}) - zQ_{cd4}] \qquad (29)$$

Where, $w = \frac{1}{2R_1}$, $z = R_1 + R_4$

The spool damping orifice is also a short tube orifice. The flow rate through this orifice is given by the following equation:

$$Q_{sd} = \frac{\pi . d_{sd}^4}{128\mu . L_{sd}}(P_s - P_{ds}) \qquad (30)$$

Where, P_{ds}, L_{sd}, and d_{sd} are valve spool downstream chamber pressure (Pa), valve spool damping hole length (m), and valve spool damping hole diameter (m), respectively.

Internal leakage in hydraulic elements is one of the problems resulting from operating at high pressure levels and the increased clearances due to wear. The leakage flow rate through the clearance between the spool and valve housing is given by:

$$Q_{Ls} = \frac{\pi . d_s C^3}{12\,\mu . L_{sh}}(P_{ds} - P_i) \qquad (31)$$

Where, L_{sh} is contact distance between valve spool and housing (m).

The leakage flow rate through the clearance between the pressure compensator and valve housing is given by:

$$Q_{Lc} = \frac{\pi . d_c C^3}{12\,\mu . L_{ch}}(P_{dc} - P_i) \qquad (32)$$

Where, L_{ch} is contact distance between compensator and housing(m).

The operating fluid, which flows from the valve spool restriction to the valve exit through the intermediate chamber, can be written as follows:

$$Q_i = C_d . A_i \sqrt{\frac{2}{\rho}(Ps - Pi)} \qquad (33)$$

Where, C_d, A_i, and ρ are discharge coefficient (---), valve spool restriction area (m^2), and oil density(kg/m^3) respectively.

The operating fluid flows from the intermediate chamber to the valve exit through compensator spool throttling. The flow rate through these restrictions, Q_m, is given by the following equation:

$$Q_m = C_d . A_o \sqrt{\frac{2}{\rho}(Pi - Pm)} \tag{34}$$

Where, A_o, is Compensator restriction area (m^2).

The continuity equation applied to the valve chambers are:

The continuity equation is applied to the intermediate chamber (I) (**Fig.2**) as follows:

$$\frac{dP_i}{dt} = (\frac{B}{V_i}) * [\, Q_i + 2Q_{cd2} + Q_{Ls} + Q_{Lc} - Q_m - Q_{cd4}] \tag{35}$$

Where, V_i , Q_i, Q_{Ls} , Q_{Lc}, *and* Q_m are Valve intermediate chamber fluid volume (m^3), Flow rate through valve spool restriction(m^3), Leakage flow rate through clearance between valve spool and valve housing(m^3), Leakage flow rate through clearance between compensator and valve housing(m^3), and, Flow rate through compensator restriction to valve exit (m^3),respectively.

The continuity equation is applied to the downstream spool spring chamber (II)(**Fig.2**) as follows:

$$\frac{dP_{ds}}{dt} = (\frac{B}{V_{bs} - As.Xs}) [\, Q_{sd} - Q_{Ls} + A_s . \frac{dX_s}{dt}] \tag{36}$$

Where, V_{bs} , and Q_{sd},Valve spool downstream chamber fluid volume (m^3),and Flow rate through valve spool damping orifice, respectively.

The continuity equation is applied to the downstream compensator spring chamber (III)(**Fig**.2) as follows:

$$\frac{dP_{dc}}{dt} = (\frac{B}{V_{bc} - A_c . X_c}) [\, Q_{cd} - Q_{Lc} + A_c \frac{dX_c}{dt}] \tag{37}$$

Where, V_{bc} , Compensator downstream chamber fluid volume (m^3).

3. SOLUTION APPROACH

Using MATLAB (SIMULINK) package 2019a, continuity equations were applied to valve chambers and valve damping holes, as well as Newton's second law on valve spool, valve core, and compensator spool. The numerical values for construction parameters, which are listed in **Table 1**, are constant inputes to the designed model. The model computed the variables listed in **Table 2** to obtain the dynamic behavior of the valve.

Table .1 Construction parameters and valve dimensions (**constants**)

Symbol	value	Unit	Symbol	value	Unit	Symbol	value	Unit
Ac	2.544e-4	m^2	K_{cs}	85000	N/m	r_i	0.003	m
As	2.544e-4	m^2	K_{se}	30000	N/m	r_o	0.007	m
B	1.9 e^9	Pa	K_{ss}	100000	N/m	V_{bc}	6.5 e-6	m^3
C	2 e^{-6}	m	L_{cd}	0.022	m	V_{bs}	9 e^{-6}	m^3
C_d	0.61	-----	L_{ch}	0.007	m	Vi	15 e^{-6}	m^3
D_c	0.018	m	L_{sd}	0.016	m	X_{co}	0.012	m
d_{cd}	0.00045	m	L_{sh}	0.007	m	X_{eo}	0.01	m
D_s	0.018	m	m_c	0.053	Kg	X_{so}	0.003	m
d_{sd}	0.002	m	m_e	0.025	kg	ρ	850	Kg/m^3
f	100	Ns/m	m_s	0.0366	Kg	μ	0.0306	Pa.s
K	10 e^9	N/m	**R**	10000	N. s/m			

Table .2 Computed parameters

Symbol	Unit		Symbol	Unit		Symbol	Unit		Symbol	Unit
A_i	m^2		F_{sc}	N		P_{dc}	Pa		Q_{Lc}	m^3/s
A_o	m^2		F_{se}	N		P_{ds}	Pa		Q_{Ls}	m^3/s
F_{bc}	N		F_{sf}	N		P_i	Pa		Q_m	m^3/s
F_{bs}	N		F_{SR1}	N		P_s	Pa		Q_{sd}	m^3/s
F_{cf}	N		F_{SR2}	N		Q_{cd1}	m^3/s		X_c	m
F_e	N		F_{SR3}	N		Q_{cd2}	m^3/s		X_e	m
F_{ef}	N		F_{SR4}	N		Q_{cd4}	m^3/s		X_s	m
F_{Ps}	N		F_{ss}	N		Q_i	m^3/s			

4. RESULTS AND DISCUSSION

The dynamic behavior of the studied valve is described by equations 1 through 37. These equations were used to develop a computer simulation program using the MATLAB (SIMULINK) package. The numerical values of the model parameter were obtained by disassembly of the valve and conducting the necessary measurements additionally manufacturer technical data sheet.
The deduced mathematical model is based on the following assumptions:

- Structure deformation under high pressure variation is not considered.
- The density and bulk modules of oil are constant.
- Variation of oil viscosity due to temperature variation is neglected.

Figure 6. Represents the effect of applying variable input current on the proportional core to steady-state valve flow rate. The supply and load pressure that are applied to the studied valve are set at 250 and zero bars, respectively. When the applied input current in the valve core increases, the controlled valve flow rate also increases, and vice versa. The half-circled machined main throttling area produces a nonlinear curve, as shown in the figure.

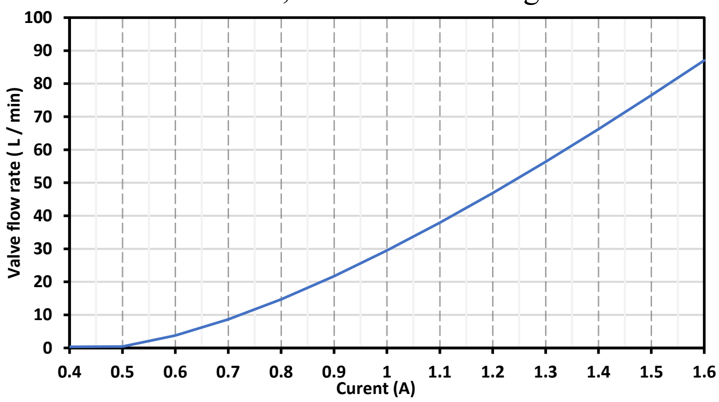

Fig.6. Variation of input current signal with valve flow rate

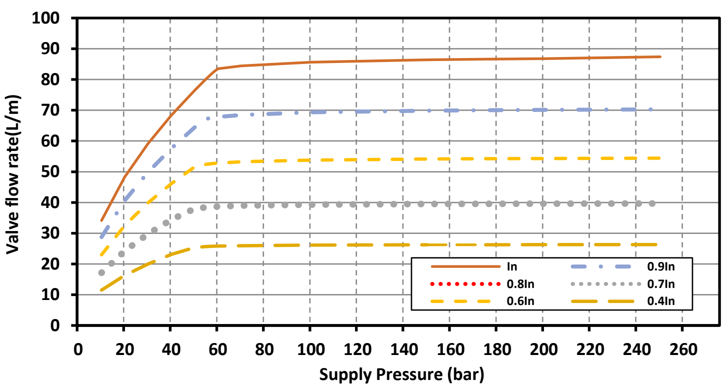

Fig.7. Effect of supply pressure variation on valve flow rate

The effect of supply pressure variation on the steady-state valve flow rate is represented in **Fig.7**. The curve is deduced by applying a constant pressure of 250 bar and zero bar at valve Inlet and exit chambers, respectively. The deduced curve is obtained at several input signals to a proportional solenoid core. The curve is divided into two zones. In the first one, the valve flow rate is uncontrolled and the valve is working as a throttling valve, whereas the supply pressure increases, which means the pressure difference also increases, and then the valve flow rate subsequently increases. At certain point, the pressure difference across the main throttling area is enough to motivate the valve compensator. At the mentioned point, the second zone has initiated. In the second zone pressure compensator, implement the function designed for it and maintain the steady-state valve flow rate almost constant regardless of the continuous rise of supply pressure.

The effect of varying the load pressure on steady-state valve flow rate is illustrated in **Fig.8**. At 100% of the input command signal applied to the proportional valve core, the studied valve is subjected to different constant supply pressures, varying the load pressure from zero bar to rated pressure. The **figure** shows that the load pressure variation doesn't affect the steady-state specified volume of flow until the pressure different force across the main throttling area can't overcome the compensator net force that applied it. At the point at which the compensator is inactive, the flow rate behavior begins to decrease until it reaches zero value at valve-rated pressure.

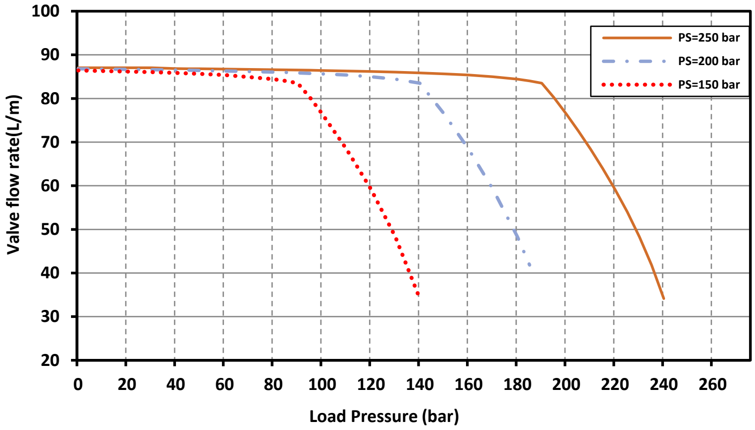

Fig.8. Effect of load pressure variation on valve flow rate

5. EXPERIMENTAL WORK

An experimental rig was designed to measure the steady-state valve flow rate under the effect of load pressure variations at different input currents applied to the valve core. The test rig is constructed in order to compare the measurements with the model results.The hydraulic test rig contains three parts (**Fig**. **9A**). The first part includes a hydraulic prime mover, a “fixed displacement gear pump driven by an electric motor “. The second one is the proportional flow control valve. The last part is the test bench. The fixed displacement pump, which is coupled with an electric motor (1) (prime mover), sucks the operating fluid from the oil tank (2) and sends it to the proportional flow control valve (3), which passes through hoses (4). The valve flow rate is measured by the flow meter (5), which is located on the test bench. To prevent the flow meter from contaminating oil, a high-pressure filter (6) must be located before the flow meter. The system load is represented by the loading valve (7). The operating fluid oil, pass through the cooler (8) during turns to the oil tank (2). Besides the flow meter, the setup is also equipped with a pressure and temperature transmitter (9).

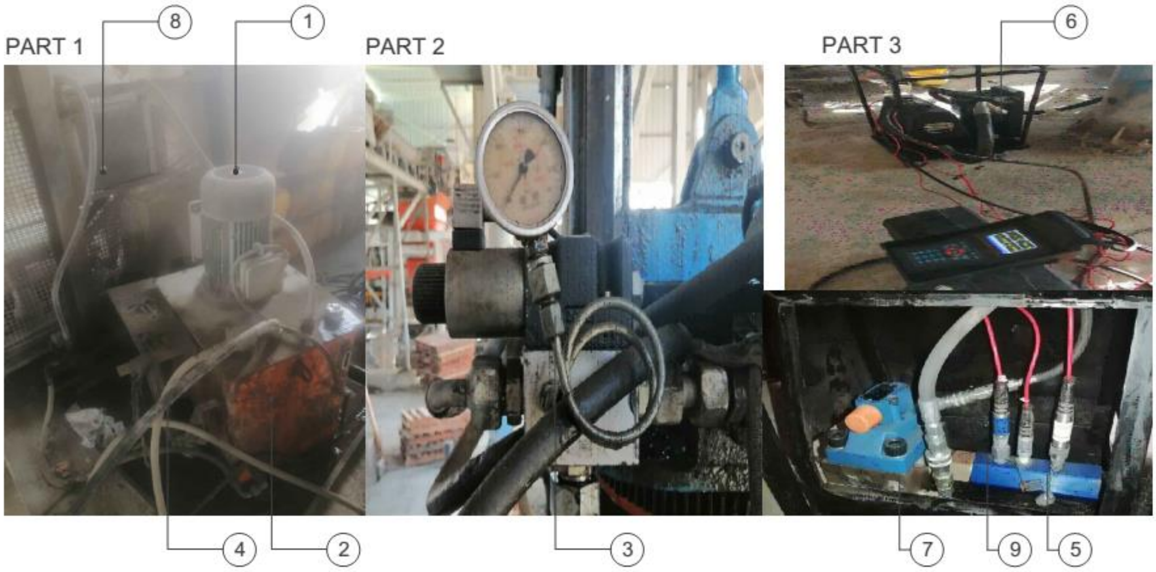

Fig.9A. Experimental setup

The hydraulic circuit, which represents the experimental setup, is illustrated in **Fig.9B**.Setting the supply pressure is achieved by a pressure relief valve, while setting the load pressure is achieved by an adjustable throttling valve.

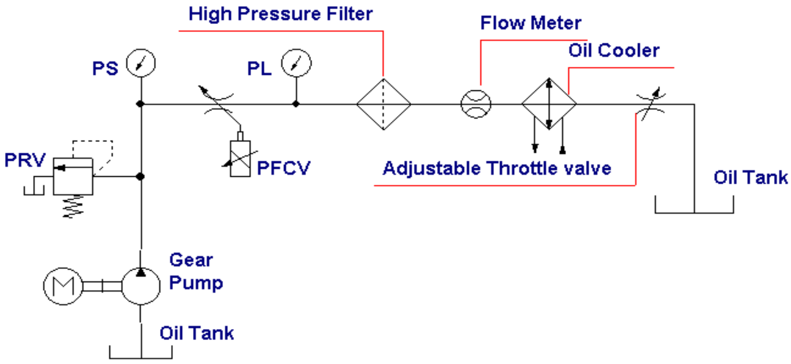

Fig.9B. Hydraulic circuit represents the experimental setup

6. MODEL VALIDATION

To verify the mathematical model represented by equations 1 through 37**,** the steady-state characteristics relation between the load pressure and the proportional valve flow rate for a constant command signal at a certain supply pressure is obtained experimentally. Several load pressure sequences were applied to the studied valve at certain input current, and a results were recorded. This experiment is repeated several available times in the same sequence at another input valve current, and the results are recorded. The experimental results compared with the mathematical model results are plotted as shown in **Figs.10A** and **10B**.

Figs.10A and **10B**, respectively, show the variation of the steady-state valve flow rate with respect to the load pressure variation. In **Fig**. **10A**, the coil is energized with (1.12 A) and the supply pressure and load pressure are set at 185 bar and zero bar, respectively. It is shown that the valve output flow is considered constant during the controlled zone regardless of load pressure variation until the pressure difference between load pressure and supply pressure is 60 bar. **Fig**. **10B** also indicates good agreement between model results and experimental results work.

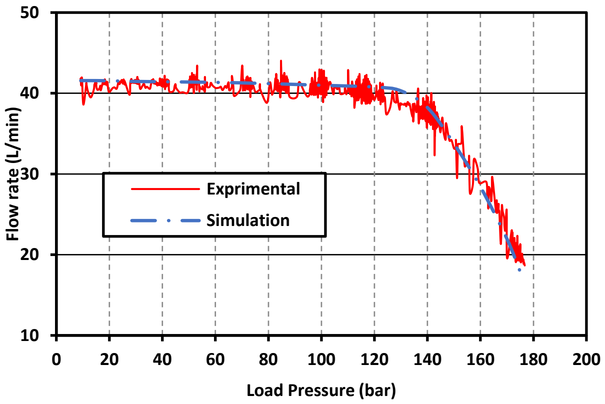

Fig.10A. Exprienmental and simulated valve flow rate to load pressure variation

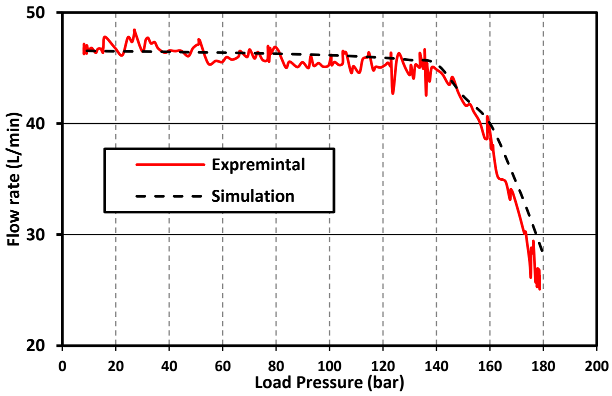

Fig.10B. Exprienmental and simuated valve flow rate to load pressure variation

To confirm the results, another command input signal of 1.2 A is applied in the core. The supply pressure and load pressure are set at 195 bar and zero bar, respectively. **Fig. 10B** shows a good match between experimental and simulated results.

7. INVESTIGATION OF THE DYNAMIC BEHAVIOR SIMULATION RESULTS

A verified simulation program is used to predict the static and dynamic behavior of the studied valve. Manufacturers can modify the studied valve characteristics by varying valve construction parameters and analyzing the obtained results.

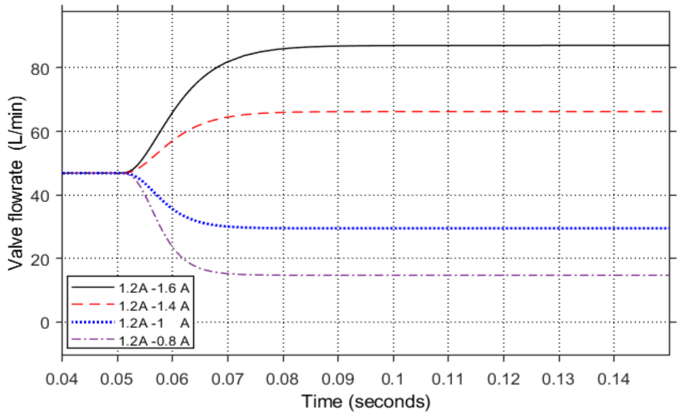

Fig.11A. Effect of input current on transient response for valve flow rate

The transient time required to give the new steady-state valve flow rate as a result of proportional coil step input current is shown in **figs. 11A** and **11B**. The current pattern presented in **Fig**. **11B** is applied to the core at 250 bar and zero bar supply and load pressures, respectively. A large step current led to an increase in the transient time, and vice versa.

Statically, load and supply pressure variations are not affected by the rate of flow of operating fluid through the studied valve. A dynamically larger step in load or supply pressure applied to the valve is required to take a long time compared to a small step to reach the new balance position again for the valve, and vice versa, as shown in **figs. 12A, 12B, and 13**.

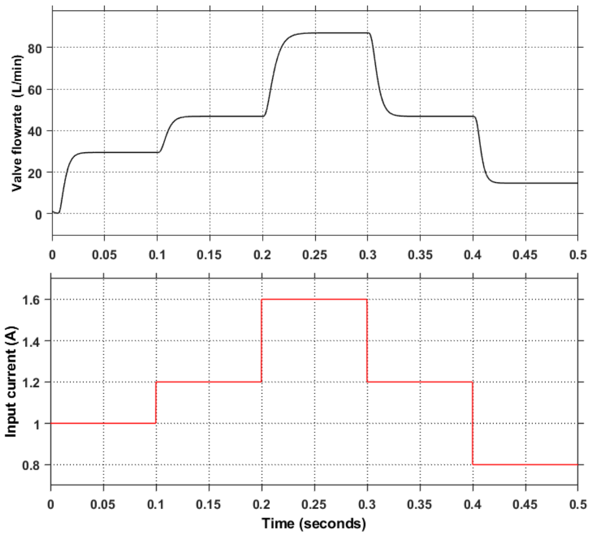

Fig.11B. Effect of certain input current pattern on transient response for valve flow rate

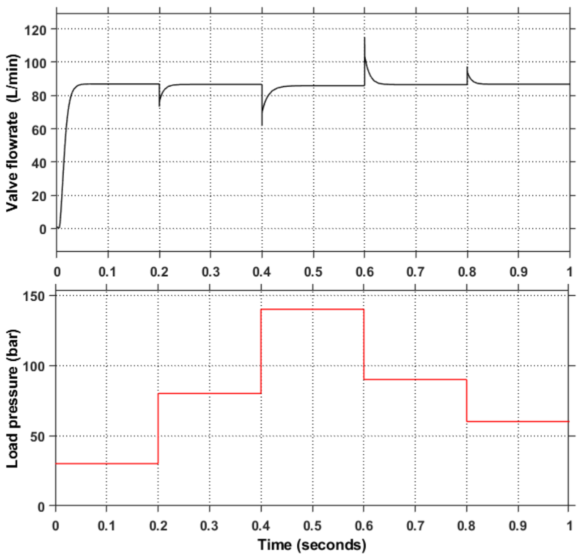

Fig.12A. Effect of a certain load pattern on transient response for valve flow rate

One of the studied parameters that controls the amount of operating fluid that passes through the main throttling area is downstream spool spring stiffness. At the rated input current that is applied to the valve coil, as the mentioned spring constant increases, the spring force that resists the solenoid force also increases. Increasing spring force leads to a decrease in the spool stroke, and lowering the main throttling area accordingly decreases the steady-state valve flow rate, as shown in **Fig.14**.

Increasing flow rate from the studied valve at a certain core input current can be achieved by increasing spring stiffness and pre-compressing displacement for the downstream compensator spring, as shown in **figs. 15A** and **16**. The amount of operating fluid flowing through the throttle valve is effected by two main parameters. The first one is the throttling area; the second one is the pressure difference across throttle. Increasing (X_{co} , K_{cs}) leads to an increase in pressure difference across the main throttling area, hence increasing the valve flow rate. The negative observation due to increasing stiffness and pre-compression is decreasing the control zone range that provides us with a constant flow rate, as shown in **Fig. 15B**.

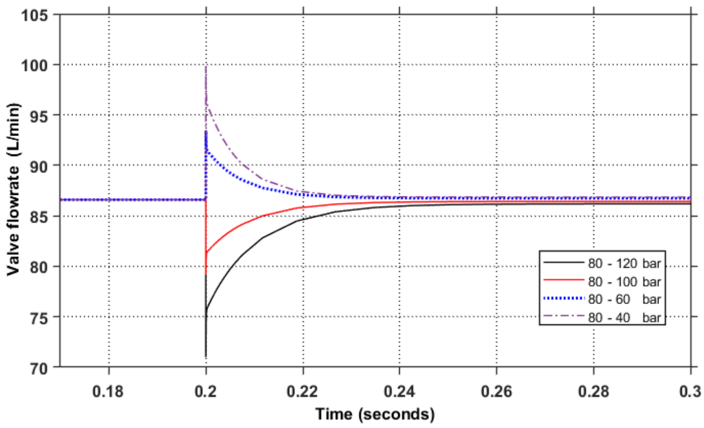

Fig.12B. Effect of load pressure variation on transient response for valve flow rate

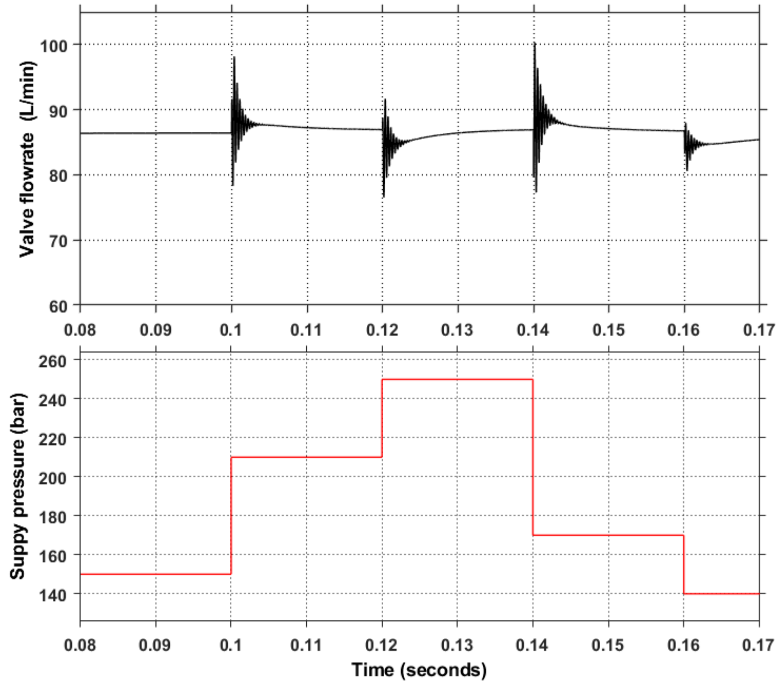

Fig.13. Effect of supply pressure variation on transient response for valve flow rate

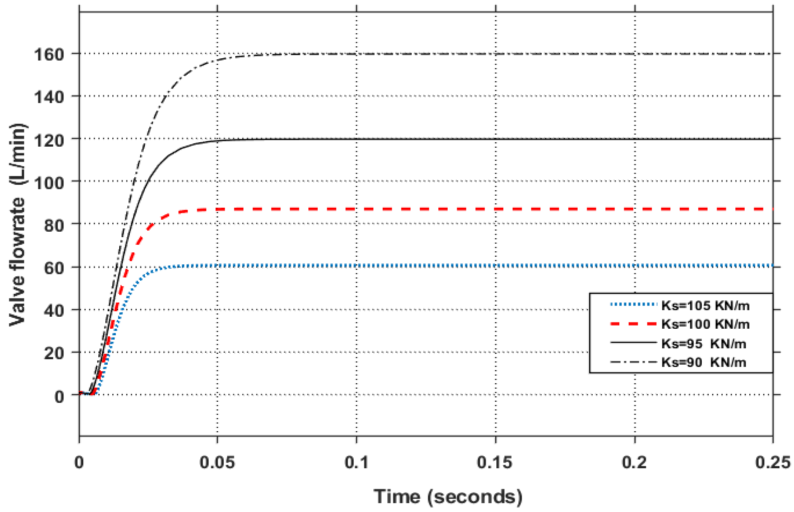

Fig.14. Effect of downstream spool spring stiffness to valve flow rate

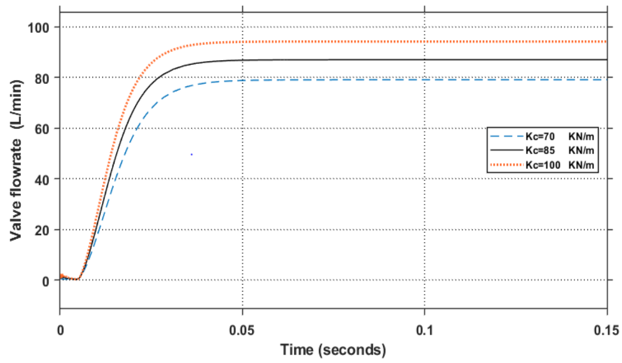

Fig.15A. Effect of downstream compensator spring stiffness on valve flow rate

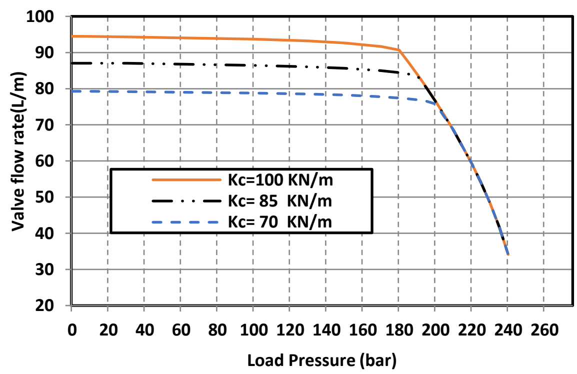

Fig.15B. Effect of downstream compensator spring stiffness on steady-state valve flow rate

The compensator spool-machined tube orifice is responsible for transferring the operating fluid between the valve inlet chamber and downstream compensator chamber. As the orifice diameter decreases, the transient response time for valve flow rate increases, and vice versa, as shown in **Fig .17**. Decreasing the orifice diameter causes an increase in resistance during traveling the operating fluid from and to the inlet and compensator downstream chambers. Increasing resistance lowers the amount of fluid through the orifice and hence increases the time needed to fill the downstream compensator chamber, subsequently lagging the steady-state new position for the valve.

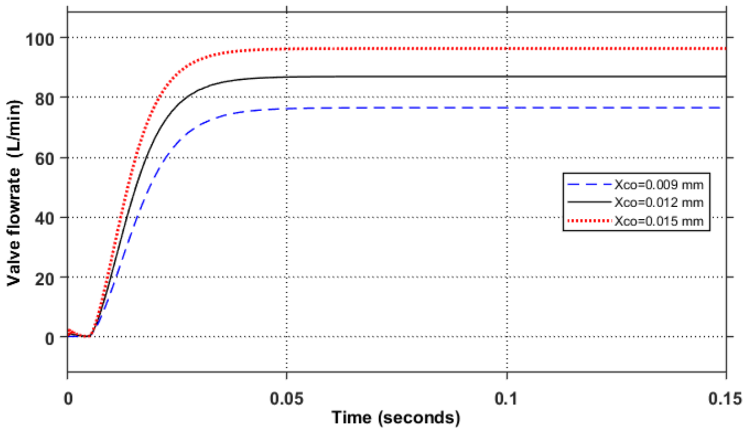

Fig.16. Effect of pre-compression for downstream compensator spring stiffness to valve flow rate

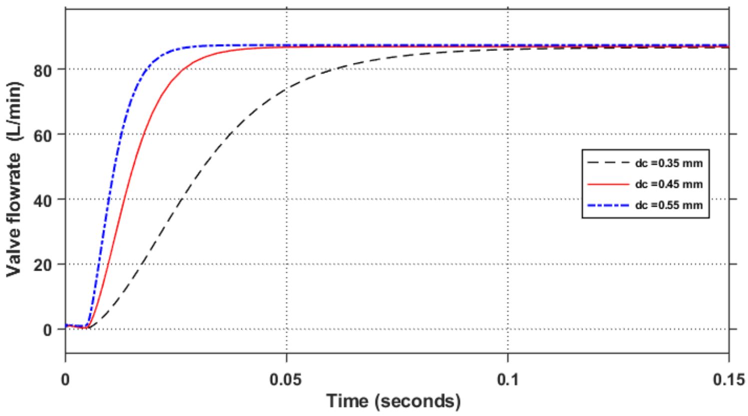

Fig.17. Effect of damping hole diameter on transient response for valve flow rate

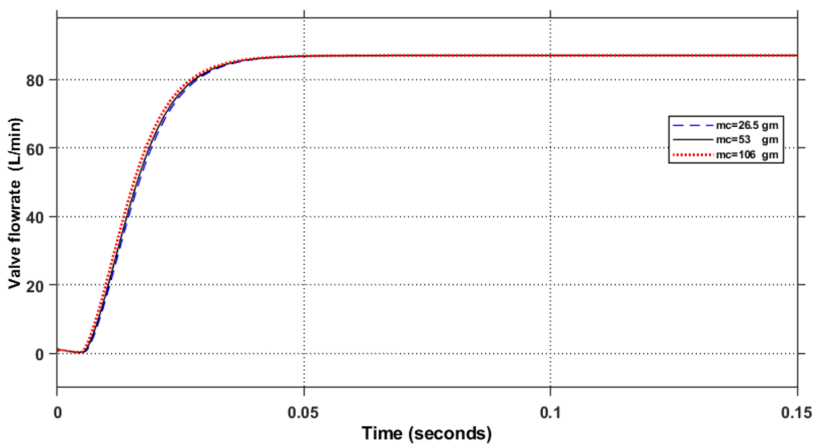

Fig.18. Effect of compensator mass on transient response time for valve flow rate

Fig.18. shows the effect of variation in compensator mass on transient time for the studied valve. Compensator mass varied between half and double value of rated mass (53 gm). The compensator inertia is not significant with respect to other forces that were applied to the compensator spool. Thus, Compensator mass variation doesn't effect on valve transient time, as presented in **Fig. 18**.

8. CONCLUSIONS

This research introduces a detailed mathematical model for a certain type of pressure-compensated proportional flow control valve. Static and dynamic behavior are investigated using a simulation program developed by the MATLAB SIMULINK package. The experimental platform is constructed to validate the steady-state valve flow rate behavior obtained from the simulation program. Simulated steady-state valve flow rate behavior closely matched that recorded from experimental work. The effect of valve spool downstream spring stiffness, compensator downstream spring stiffness(), pre-compression for compensator downstream spring,compensator mass, and compensator damping hole diameter are studied .Results indicate that ,

1- The existence of the studied valve family before actuators in hydraulic circuits guarantees several auto-controlled constant flow rates during the controlled zone, regardless of operating condition variation.
2- An increase in pre-compression and spring stiffness located in the compensator downstream chamber increases the valve flow rate but decreases the transient time and controlled zone range.
3- An increase in valve spring stiffness decreases the flow rate .
4- Increasing compensator damping orifice diameter decreases transient time.
5- Compansator mass has no significant impact on the transient time.
6- Another marked point is that transient response time increases with a large step change in input command value, load pressure, and supply pressure applied to the studied valve.

NOMENCLATURE

A_c	Compensator cross section area	m^2
A_i	Valve spool restriction area	m^2
A_o	Compensator restriction area	m^2
A_s	Valve spool cross section area	m^2
B	Bulk modulus of oil	Pa
C	Clearance between valve spool and housing	m
C_d	Discharge coefficient	-----
D_c	Compensator diameter	m
d_{cd}	Diameter of compensator damping orifice	m
D_s	Valve spool diameter	m
d_{sd}	Diameter of valve spool damping orifice	m
f	Friction coefficient	N.s/m
F_{bc}	Downstream pressure force applied in Compensator	N
F_{bs}	Downstream pressure force applied in valve spool	N
F_{cf}	Viscous friction force for compensator	N
F_e	Solenoid force applied on core	N
F_{ef}	Viscous friction force for core	N
F_{Ps}	Upstream pressure force applied in valve spool	N
F_{sc}	Compensator spring force	N

F_{se}	Core spring force	N
F_{sf}	Viscous friction force for valve spool	N
F_{SR1}	Seat reaction force produced by seating the core in core housing	N
F_{SR2}	Seat reaction force produced by seating the valve spool in valve housing	N
F_{SR3}	Contact force produced by seating the valve spool on core	N
F_{SR4}	Seat reaction force produced by seating the compensator in valve housing	N
F_{ss}	Valve spool spring force	N
I	PFCV input current	A
K	Equivalent seat material stiffness	N/m
K_{cs}	Downstream Compensator spring stiffness	N/m
K_{se}	Core spring stiffness	N/m
K_{ss}	Downstream valve spool spring stiffness	N/m
L_{cd}	Length of compensator damping orifice	m
L_{ch}	Contact distance between compensator and housing	m
L_{sd}	Length of valve spool damping orifice	m
L_{sh}	Contact distance between valve spool and housing	m
m_c	Compensator mass	Kg
m_e	Core mass	kg
m_s	Valve spool mass	Kg
P_{dc}	Pressure in downstream Compensator chamber	Pa
P_{ds}	Downstream pressure applied on valve spool	Pa
P_i	Pressure in intermediate chamber for valve	Pa
P_s	Upstream pressure applied in valve spool	Pa
Q_{cd}	Flow rate through compensator damping orifice	m^3/s
Q_i	Flow rate through valve spool restriction	m^3/s
Q_{Lc}	Leakage flow rate through clearance between compensator and valve housing	m^3/s
Q_{Ls}	Leakage flow rate through clearance between valve spool and valve housing	m^3/s
Q_m	Flow rate through compensator restriction to valve exit	m^3/s
Q_{RV}	Flow rate through PRV	m^3/s
Q_{sd}	Flow rate through valve spool damping orifice	m^3/s
R	Equivalent seat material damping coefficient	N. s/m
r_i	Radius of spool orifice area	m
r_o	Radius of compensator orifice area	m
V_{bc}	Compensator downstream chamber fluid volume	m^3
V_{bs}	Valve spool downstream chamber fluid volume	m^3
V_i	Valve intermediate chamber fluid volume	m^3
X_c	Compensator displacement	m
X_{co}	Initial downstream Compensator spring	m
X_e	Core displacement	m
X_{eo}	Downstream core spring pre-compression	m
X_s	Valve spool displacement	m
X_{so}	downstream valve spring pre-compression	m
μ	Oil dynamic viscosity coefficient	Pa.s

REFERENCES

[1] Li Y., Li R., Yang J., Yu X.,Xu,and J.(2023). Review of Recent Advances in the Drive Method of Hydraulic Control Valve. Processes, 11,2537. https://doi.org/10.3390/pr11092537.

[2] Bury P., Stosiak M., Urbanowicz K., Kodura A., Kubrak M., and Malesinska A.(2022). A Case Study of Open- and Closed-Loop Control of Hydrostatic Transmission with Proportional Valve Start-Up Process. Energies , 15, 1860. https://doi.org/10.3390/en15051860.

[3] Xu B., Shen J., Liu S., Su Q., Zhang, and J.(2020). Research and Development of Electro-Hydraulic Control Valves Oriented to Industry. Chin. J. Mech. Eng., 33, 29.

[4] Paolo T., Andrew R., Elia D.,and Riccardo A.(2018).Review of Direct Drive Proportional Electrohydraulic Spool Valves: Industrial State-of-The-Art and Research Advancements. Journal of Dynamic Systems, Measurement and Control, doi:10.1115/1.4041063.

[5] Majid D., Afshine I., Senior M.,Masoud V.,and Sohel A. (2013).A Hydraulic Wind Power Transfer System: Operating And Modeling. IEEE Transactions on Industry Applications.

[6] Majid D., Afshine I., Senior M.,Masoud V.,and Sohel A.(2015). Modeling of a hydraulic wind power transfer system utilizing a proportional flow control valve. IEEE Transactions on Industry Applications, 51(2): 1837–1844

[7] Alessandro F., Pietro P., and Massimo R.(2018). Modelling and Experimental Studies on A Proportional Valve Using an Innovative Dynamic Flow-Rate Measurement in Fluid Power Systems. Mechanical Engineering Science, doi: 10.1177/0954406217721259.

[8] Wang H., Wang X., and Huang J. (2020). Flow Control for a Two-Stage Proportional Valve with Hydraulic Position Feedback. Chin. J. Mech. Eng. 33, 93 .

[9] Edward L. , and Grzegorz F. (2016) .Modelling and Experimental Studies on A Proportional Valve Using an Innovative Dynamic Flow-Rate Measurement in Fluid Power Systems. Energy Conversion and Management, Volume 123, Pages 15-28.

[10] He W. ,Xiaohu W., and Jiahai H. (2018). A Novel Control Strategy for Pilot Controlled Proportional Flow Valve With Internal Displacement-Flow Feedback. Journal of Dynamic Systems, Measurement, and Control, Vol. 140/ 111014-1, doi: 10.1115/1.4040328.

[11] D.Wu , R.Burton ,G.Schoenau, and D.Bitner (2007) .Analysis of Pressure-Compensated Flow Control Valve. Journal of dynamic systems, measurement ,and control, vol.129,pp.203-211.

[12] Don D. (2003) .Proportional and Servo Technology" Fluid power journal, pp.8-12.

[13] Mannesmann Rexroth GmbH .Basic principle and components of fluid technology. The hydraulic trainer volume 1, RE00290/10.91,199

[14] Mannesmann Rexroth GmbH .Proportional and servo technology. The hydraulic trainer volume 2, RE00291/12.89.

[15] Minter Cheng (2005) .Modeling and Analysis of A Pressure Compensated Flow Control Valve. Proceeding of FEDSM2005,ASME,Fluid engineering division summer meeting,Houston ,Texas ,USA,Volume 2,pp.17-25.

[16] M.Galal Rabie,(2009) .Fluid Power Engineering. McGraw-Hill, New York.

[17] M. Gomaa , Ziad A. , and M.Elfaisal(2023).Design, Modeling, Simulation and Investigation of the Dynamic Behavior of a Hydrostatic Power Transmission System for Horizontal Axis Wind Turbine. Journal of Al-Azhar University Engineering Sector, vol. 19, Issue70, 2023.

[18] https://duplomaticmotionsolution.com.

[19] Shijie W., Zhidan W. ,and Bo.Jin (2020) .A Performance Improvement Strategy For Solenoid Electromagnetic Actuator in Servo Proportional Valve. Appl.sci ,10,4352.

[20] M.F. Badr (2018) .Modeling and simulation of a control solenoid" IOP Conf .series :Material science and engineering 433(2018)012082 .

[21] Masruki K., Made., Bambang P., and Agus P.(2016) . Modelling and Simulation Analysis of Solenoid Valve For Spring Constant Influenceto Dynamic Response. ARPN Journal of Engineering and Applied Sciences, vol. 11, no. 4.